ISSN 0036-0236, Russian Journal of Inorganic Chemistry, 2020, Vol. 65, No. 5, pp. 663–667. © Pleiades Publishing, Ltd., 2020.
Russian Text © The Author(s), 2020, published in Zhurnal Neorganicheskoi Khimii, 2020, Vol. 65, No. 5, pp. 613–618.

THERMODYNAMICS OF INORGANIC COMPOUNDS

# Effects of Rare-Earth Metals on the Thermal Stability and Glass-Forming Ability of Al–Ni–Co–R Amorphous Alloys

**B. A. Rusanov[a, *], V. E. Sidorov[a, b], P. Svec, Sr.[c], P. Svec[c], and D. Janickovic[c]**

[a] *Ural State Pedagogical University, Yekaterinburg, 620017 Russia*
[b] *Ural Federal University, Yekaterinburg, 620002 Russia*
[c] *Institute of Physics, Academy of Sciences of Slovakia, Bratislava, 84511 Slovakia*
**e-mail: rusfive@mail.ru*

Received November 6, 2019; revised November 24, 2019; accepted December 27, 2019

**Abstract**—$Al_{86}Ni_4Co_4R_6$ and $Al_{86}Ni_6Co_2R_6$ (R = Nd, Sm, Gd, Tb, or Yb) metallic ribbons were produced by planar flow spin casting. The glass-transition and phase-transformation temperatures of these alloys were determined in crystallization kinetic studies. Glass-forming criteria for these alloys were calculated from differential scanning calorimetry (DSC) and differential thermal analysis (DTA) data. The rare-earth metals and combinations of transition metals useful to enhance the thermal stability and glass-forming ability of the alloys were found.

**Keywords:** aluminum alloys, amorphous alloys, glass-forming ability, rare-earth metals, structure
**DOI:** 10.1134/S0036023620050198

## INTRODUCTION

The development of aircraft, rocket, and shipbuilding requires technologists to provide new materials with improved mechanical characteristics, corrosion resistance, unique electrical and magnetic properties. The existing crystalline (even though multicomponent) alloys do not satisfy these requirements. One way out is to use amorphous metal alloys. Amorphous and nanocrystalline aluminum alloys with 3*d*-transition and rare-earth metals are items with perfect mechanical and corrosion properties [1–5]. Where the transition metal is nickel, alloys show enhanced microhardness and tensile strength [1]. Cobalt-doped alloys are distinguished by high corrosion resistance, being regarded as candidate protective coatings [6]. However, the compositions and preparation methods for amorphous metallic alloys are selected empirically due to the nonexistence of theory that would explain the high glass forming ability (GFA) of aluminum alloys doped with 3*d* and rare-earth metals.

Our previous studies showed that a combination of nickel and cobalt provides amorphous Al–Ni–Co–R alloys with higher thermal stability compared to ternary systems [7, 8]. Here we present the results of thermoanalytical experiments on aluminum metallic glasses containing various amounts of 3*d* metals and various rare-earth metals. These results were used to calculate the glass-forming criteria for Al–Ni–Co–R alloys; the effects of various rare-earth metals on the thermal stability and glass-forming ability of the alloys were analyzed.

## EXPERIMENTAL

The initial alloys $Al_{86}Ni_4Co_4R_6$ and $Al_{86}Ni_6Co_2R_6$ (R = Nd, Sm, Gd, Tb, and Yb) were produced by alloying pure metals in an induction furnace for 0.5 h at 1923 K under an argon atmosphere. The chemical compositions of alloys were analyzed using an atomic-adsorption spectrometer. Amorphous ribbons (width—3 mm and thickness—39–45 μm) were produced by standard planar flow casting under a controlled inert gas atmosphere. The cell was degassed and then filled with argon to $10^3$ Pa. The melt was overheated up to 1500–1523 K and then injected to a water-cooled copper wheel. The amorphous structure of ribbons was verified by X-ray diffraction ($CuK_\alpha$ radiation) on a Bruker D8 Advance diffractometer.

The crystallization kinetics and thermal stability were studied by differential scanning calorimetry (DSC) and differential thermal analysis (DTA) on Perkin-Elmer DSC-7 and Perkin-Elmer DTA-7, respectively. DTA experiments were carried out under an argon atmosphere (flow rate: 20 mL/min). The heating rate in experiments was 20 K/min. Prior to DTA experiments the setup was calibrated against the aluminum and gold melting points. Characteristic temperatures were determined in Pyris Data Analysis software intended for analyzing data from Perkin-Elmer instruments.

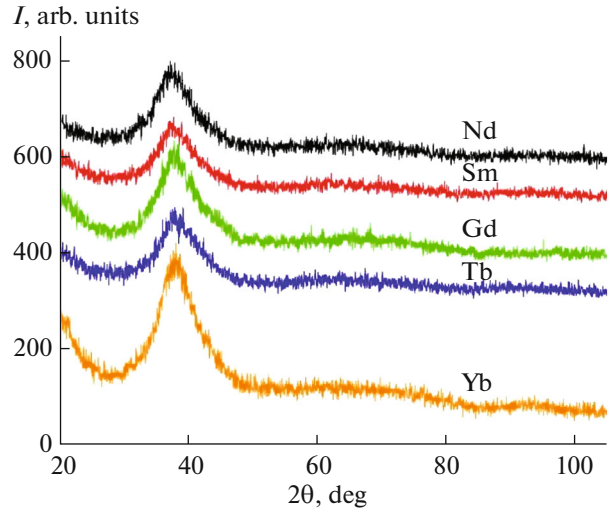


**Fig. 1.** X-ray diffraction curves for $Al_{86}Ni_4Co_4R_6$ ribbons. Curves are shifted up along the vertical axis for clarity.

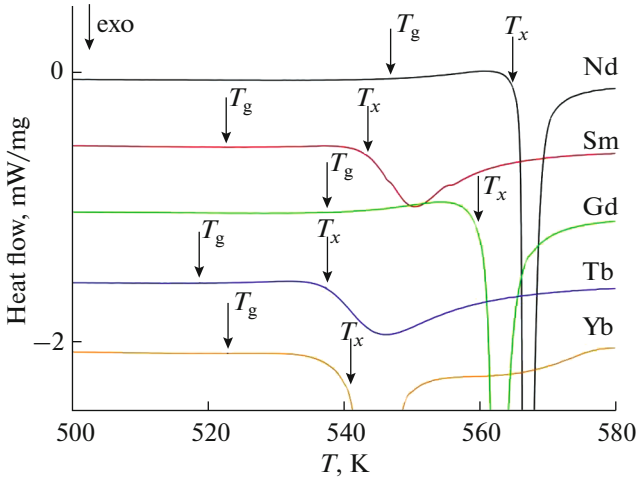


**Fig. 2.** DSC curves for $Al_{86}Ni_4Co_4R_6$ alloys obtained at the 20 K/min heating rate. Curves are shifted down along the vertical axis for clarity (for the samarium alloy, by 0.5 units; for the gadolinium alloy, by 1 unit; for the terbium alloy, by 1.5 units; and for the ytterbium alloy, by 2 units).

## RESULTS AND DISCUSSION

All ribbons were amorphous to X-rays (Fig. 1). Representative DSC curves are shown in Figs. 2 and 3.

All alloys containing 4 at % nickel and 4 at % cobalt featured a glass-transition point ($T_g$) and a quite extensive area of "undercooled liquid" (suspended between the glass-transition point $T_g$ and the crystallization onset point $T_x$), which is not typical of amorphous aluminum-based alloys. This fact can serve as evidence for combinations of 3*d*-transiiton metals and rare-earth metals endowing alloys with a high tendency to amorphization.

The $T_g$ and $T_x$ for all rare-earth metals have rather close values within the span of 30 K. The highest thermal stability is observed for neodymium and gadolinium alloys. The $T_g$ and $T_x$ are 547, 565 K for neodymium alloys and 539, 560 K for gadolinium alloys. Samarium, terbium, and ytterbium alloys have lower glass-transition and crystallization onset temperatures. This can be due to Sm, Tb, and Yb in multicomponent alloys having a variable valence; that is, prototypes of intermetallic compounds, which are not typical of neodymium and gadolinium alloys, appear in the amorphous phase. These compounds, as a rule, are metastable and appear in the first crystallization stage [9].

The DSC results for alloys containing 6 at % nickel and 2 at % cobalt are shown in Fig. 3.

There are two noteworthy distinctions between DSC curves for these compositions. Firstly, for samarium and ytterbium alloys glass-transition points are not detected even at high heating rates (40 K/min). Secondly, the nickel amount in alloys increasing to 6 at % decreases the glass-transition temperature ($T_g$) and crystallization onset temperature ($T_x$) by 20–40 K for all rare-earth metals. Neodymium and gadolinium alloys yet have the highest thermal stability, though the terbium alloy has approached them.

Summarizing DSC results for alloys of various compositions, we observed that equal amounts of nickel and cobalt in alloys are most preferable in the context of enhancing the thermal stability of the alloys.

In order to have a more intimate insight into the crystallization of amorphous ribbons, identify solidus

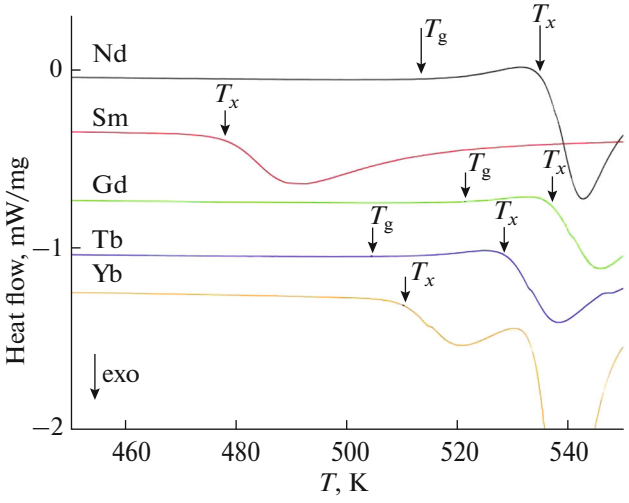


**Fig. 3.** DSC curves for $Al_{86}Ni_6Co_2R_6$ alloys obtained at the 20 K/min heating rate. Curves are shifted down along the vertical axis for clarity (for the samarium alloy, by 0.3 units; for the gadolinium alloy, by 0.7 units; for the terbium alloy, by 1 unit; and for the ytterbium alloy, by 1.25 units).

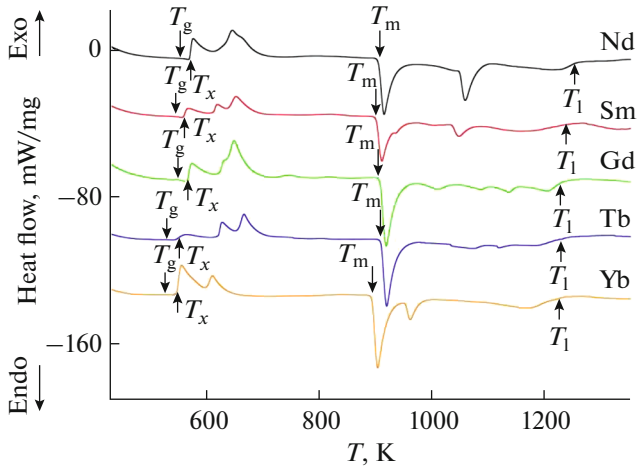


**Fig. 4.** DTA curves for $Al_{86}Ni_4Co_4R_6$ alloys obtained at the 20 K/min heating rate. Curves are shifted down along the vertical axis for clarity (for the samarium alloy, by 37 units; for the gadolinium alloy, by 60 units; for the terbium alloy, by 100 units; and for the ytterbium alloy, by 130 units).

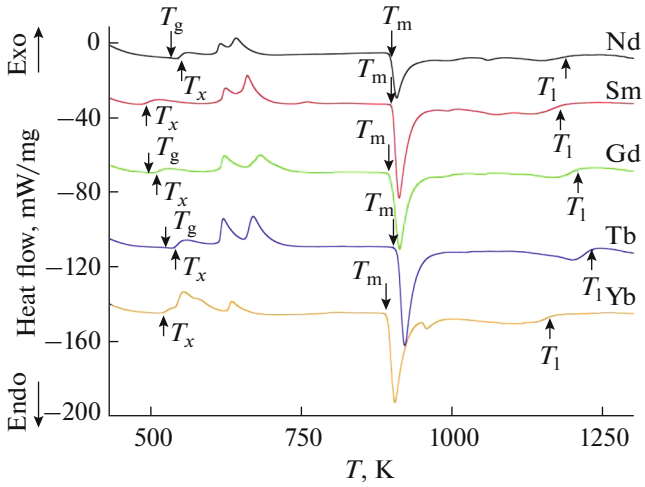


**Fig. 5.** DTA curves for $Al_{86}Ni_6Co_2R_6$ alloys obtained at the 20 K/min heating rate. Curves are shifted down along the vertical axis for clarity (for the samarium alloy, by 30 units; for the gadolinium alloy, by 65 units; for the terbium alloy, by 105 units; and for the ytterbium alloy, by 140 units).

and liquidus temperatures, and further calculate glass-forming parameters, we carried out a series of DTA. Representative results for alloys containing 4 at % nickel and 4 at % cobalt are shown in Fig. 4.

The crystallization of amorphous ribbons that contain 4 at % nickel and 4 at % cobalt was found to occur, as a rule, in three stages, in good agreement with our previous studies [7–9]. Apart from the major phases (Al, $Al_9Co_2$, $Al_3Ni$, $Al_3R$, and $Al_{11}R_3$), ternary stable and metastable compounds like $Al_{19}Ni_5R_3$ and $Al_{23}Ni_6R_4$ can appear; however, this is beyond discussion here.

Melting for all compositions occurs in several stages and has an extensive (more than 300 K) two-phase area. For the solidus temperatures, a nonlinear variation is observed with a 909-K peak for terbium. This situation is typical of alloys where the rare-earth metal is used in low concentrations. As a rule, characteristic temperatures (in the case at hand, solidus temperatures) reach an extreme in the middle of the series. Noteworthy, for gadolinium alloys the solidus is at a close temperature (907 K), thereby providing one more piece of evidence for this rule within the error bar of DTA temperature determination. As to the liquidus temperature, it decreases monotonically from 1257 K in the neodymium alloy to 1233 K in the ytterbium alloy.

Figure 5 shows DTA results for alloys containing 6 at % nickel and 2 at % cobalt.

Devitrification in these alloys has a more intricate pattern than in 4 × 4 alloys. This process is accompanied by three or four (in the samarium alloy) exotherms.

In the two-phase area between the solidus and liquidus, however, no significant thermal events appear; this area also has an appreciable temperature extent (of about 300 K). The solidus and liquidus temperatures themselves well correlate with each other and have maximum values for terbium- and gadolinium-containing alloys.

We used the characteristic temperatures for Al–Ni–Co–R alloys written from DSC and DTA curves to calculate the best-known glass-forming ability (GFA) criteria [10–19]. One of the most common criteria is $T_{rg} = T_g/T_l$; in order to calculate it, one is to use the glass-transition temperature $T_g$ and the liquidus temperature $T_l$ [10–12]. As a rule, calculations of other criteria also require one to know the glass-transition temperature ($T_g$): $\Delta T_x = T_x - T_g$ [13], $\gamma = T_x/(T_g + T_l)$ [14], $\delta = T_x/(T_l - T_g)$ [15], $\beta = (T_gT_x)/(T_l + T_x)2$ [16], $\gamma_m = (2T_x - T_g)/T_l$ [17], $\gamma_c = (3T_x - 2T_g)/T_l$ [18], and $\xi = (T_g/T_l) + (\Delta T_x/T_x)$ [19], where $T_x$ is the crystallization onset temperature of the amorphous alloy and $T_l$ is the melting (liquidus) temperature.

The characteristic temperatures and results of calculation appear in Table 1. The values of γ, δ, and β for the studied alloys well agree with the results of calculation for other amorphous aluminum alloys (see, e.g., calculations in [20]).

At the same time, it can be seen that the existing criteria in no way reflect the change in the glass-forming ability of Al–Ni–Co–R alloys due to alloying with various rare-earth metals, although we found this experimentally. Therefore, it is necessary to introduce a new criterion that would eliminate these disadvantages, and this criterion should contain information about the state of the melt before quenching.

**Table 1.** Characteristic temperatures of Al–Ni–Co–R amorphous alloys as determined by DSC and DTA (heating rate: 20 K/min) and the results of calculation of glass-forming ability parameters

| Alloy | $T_g$ | $T_x$ | $T_m$ | $T_l$ | $T_{rg}$ | $\Delta T_x$ | γ | δ | β | $\gamma_m$ | $\gamma_c$ | ξ |
|---|---|---|---|---|---|---|---|---|---|---|---|---|
| | K | | | | | | | | | | | |
| $Al_{86}Ni_4Co_4Nd_6$ | 547 | 565 | 904 | 1257 | 0.44 | 18 | 0.31 | 0.80 | 0.09 | 0.46 | 0.48 | 0.47 |
| $Al_{86}Ni_4Co_4Sm_6$ | 522 | 543 | 900 | 1244 | 0.42 | 21 | 0.31 | 0.75 | 0.09 | 0.45 | 0.47 | 0.46 |
| $Al_{86}Ni_4Co_4Gd_6$ | 539 | 560 | 907 | 1236 | 0.44 | 21 | 0.32 | 0.80 | 0.09 | 0.47 | 0.49 | 0.47 |
| $Al_{86}Ni_4Co_4Tb_6$ | 518 | 537 | 909 | 1234 | 0.42 | 19 | 0.31 | 0.75 | 0.09 | 0.45 | 0.47 | 0.46 |
| $Al_{86}Ni_4Co_4Yb_6$ | 523 | 543 | 893 | 1233 | 0.42 | 20 | 0.31 | 0.77 | 0.09 | 0.46 | 0.47 | 0.46 |
| $Al_{86}Ni_6Co_2Nd_6$ | 517 | 535 | 896 | 1203 | 0.43 | 18 | 0.31 | 0.78 | 0.09 | 0.46 | 0.47 | 0.46 |
| $Al_{86}Ni_6Co_2Sm_6$ | – | 478 | 900 | 1188 | – | – | – | – | – | – | – | – |
| $Al_{86}Ni_6Co_2Gd_6$ | 522 | 540 | 898 | 1212 | 0.43 | 18 | 0.31 | 0.78 | 0.09 | 0.46 | 0.48 | 0.46 |
| $Al_{86}Ni_6Co_2Tb_6$ | 512 | 529 | 908 | 1235 | 0.42 | 17 | 0.30 | 0.73 | 0.09 | 0.44 | 0.46 | 0.45 |
| $Al_{86}Ni_6Co_2Yb_6$ | – | 510 | 892 | 1168 | – | – | – | – | – | – | – | – |

However, there is another way to solve the problem, namely, studying the physical and chemical properties of Al–Ni–Co–R melts. In this case, it is possible to predict the effect of the alloying element on the glass-forming ability (GFA) without manufacturing the amorphous ribbons themselves. For example, we have shown that the paramagnetic Curie temperature determined from the temperature-dependent magnetic susceptibility of melts can be a good criterion. If the additive enhances the interatomic interaction in the melt (increases the paramagnetic temperature θ), then it will increase the GFA of the alloys; if it decreases θ, then it will adversely affect and the glass-forming ability of alloys [21].

## CONCLUSIONS

The crystallization kinetic studies of amorphous Al–Ni– Co–R alloys with various rare-earth metals have shown that the alloys typically have a supercooled liquid field and a glass-transition point (which is not typical of amorphous aluminum-based alloys) and a high thermal stability. The calculated GFA criteria indicate that these alloys exhibit a high tendency to glass formation. However, these criteria do not allow one to unambiguously decide which of the rare-earth elements is preferable.

A combination of 4 at % nickel and 4 at % cobalt is preferable for producing amorphous Al–Ni–Co–R alloys, due to it providing alloys highly prone to amorphization. A detailed study of the effects of various rare-earth metals on the characteristic temperatures of these alloys has shown that neodymium, gadolinium, and terbium are the best dopants in terms of increasing glass-transition, crystallization onset, and melting temperatures.

## ACKNOWLEDGMENTS

B. Rusanov is grateful to the Slovak Academic Information Agency (SAIA).

## FUNDING

The study was supported by VEGA project nos. 2/0082/17 and APVV-15-0049.

## CONFLICT OF INTEREST

The authors declare that they have no conflict of interest.

## REFERENCES

1. A. Inoue, K. Ohtera, A. P. Tsai, et al., Jpn. J. Appl. Phys. **27**, L479 (1988). https://iopscience.iop. org/article/10.1143/JJAP.27.L479.
2. T. Gloriant and A. L. Greer, Nanostruct. Mater. **10**, 389 (1998). https://doi.org/10.1016/S0965-9773(98)00079-8
3. C. Rios, M. D. Bary, et al., J. Non-Cryst. Solids **354**, 4874 (2008). https://doi.org/10.1016/j.jnoncrysol.2008.04.035
4. Y. Ouyang, J. Zhang, H. Chen, et al., J. Alloys Compd. **454**, 359 (2008). https://doi.org/10.1016/j.jallcom.2006.12.088
5. W. J. Botta, R. C. Triveno, R. D. SaLisboa, et al., J. Alloys Compd. **483**, 89 (2009). https://doi.org/10.1016/j.jallcom.2008.08.122
6. C. L. Li, P. Wang, S. Q. Sun, et al., Appl. Surf. Sci. **384**, 116 (2016). https://doi.org/10.1016/j.apsusc.2016.04.188
7. B. Rusanov, V. Sidorov, P. Svec, Sr., et al., J. Alloys Compd. **787**, 448 (2019). https://doi.org/10.1016/j.jallcom.2019.02.058
8. B. Rusanov, V. Sidorov, P. Svec, et al., Tech. Phys. **64**, 1488 (2019). https://doi.org/10.1134/S1063784219100190

9. V. Sidorov, S. Petrova, P. Svec, Sr., et al., EPJ Spec. Topics **226**, 1107 (2017). https://doi.org/10.1140/epjst/e2016-60226-x
10. S. Guo, Z. P. Lu, and C. T. Liu, Intermet **18**, 883 (2010). https://doi.org/10.1016/j.intermet.2009.12.025
11. Z. P. Lu, H. Bei, and C. T. Liu, Intermet **15**, 618 (2007). https://doi.org/10.1016/j.intermet.2006.10.017
12. D. Turnbull, Contemp. Phys. **10**, 473 (1969). https://doi.org/10.1080/00107516908204405
13. A. Inoue, T. Zhang, and T. Masumoto, Mater. Trans. JIM **31**, 177 (1990). https://doi.org/10.2320/matertrans1989.31.177
14. Z. P. Lu and C. T. Liu, Acta Mater. **50**, 3501 (2002). https://doi.org/10.1016/S1359-6454(02)00166-0
15. Q. J. Chen, J. Shen, D. Zhang, et al., Mater. Sci. Eng. A **433**, 155 (2006). https://doi.org/10.1016/j.msea.2006.06.053
16. Z. Z. Yuan, S. L. Bao, Y. Lu, et al., J. Alloys Compd. **459**, 251 (2008). https://doi.org/10.1016/j.jallcom.2007.05.037
17. X. H. Du, J. C. Huang, C. T. Liu, et al., J. Appl. Phys. **101**, 086108 (2007). https://doi.org/10.1063/1.2718286
18. S. Guo and C. T. Liu, Intermet **18**, 2065 (2010). https://doi.org/10.1016/j.intermet.2010.06.012
19. X. H. Du and J. C. Huang, Chine. Phys. B **17**, 249 (2008). https://doi.org/10.1088/1674-1056/17/1/043
20. J. Zhang, P. Shi, and A. Chang, J. Non-Cryst. Solids **1**, 100005 (2019). https://doi.org/10.1016/j.nocx.2018.100005
21. V. E. Sidorov, V. A. Mikhailov, and A. A. Sabirzyanov, Russ. Metall. (Metally), No. 2, 109 (2016). https://doi.org/10.1134/S0036029516020166

*Translated by O. Fedorova*